MRA DATA SEGMENTATION USING LEVEL SETS

Hossam Hassan and Aly A. Farag
Computer Vision and Image Processing Lab,
University of Louisville, Louisville, KY 40292.
{hossam, farag}@cvip.louisville.edu
http://www.cvip.uofl.edu

ABSTRACT

In this paper, we use a level set based segmentation algorithm to extract the vascular tree from Magnetic Resonance Angiography, "MRA". Classification model finds an optimal partition of homogeneous classes with regular interfaces. Regions and their interfaces are represented by level set functions. The algorithm initializes level sets in each image slice using automatic seed initialization and then iteratively, each level set approaches the steady state and contains the vessel or non-vessel area. The algorithm is applied on each slice of the volume to build up the tree. The results are validated using a phantom that simulates the "MRA". The approach is fast and accurate. Results on various cases demonstrate the accuracy of the approach.

Keywords: Level Set Segmentation, Vascular Tree, Seed Initialization, MRA, PDE.

1. INTRODUCTION

The human cerebrovascular system is a complex three-dimensional anatomical structure. Serious types of vascular diseases such as carotid stenosis, aneurysm, and vascular malformation may lead to brain stroke, which are the third leading cause of death and the number one cause of disability. An accurate model of the vascular system from MRA data volume is needed to detect these diseases at early stages and hence may prevent invasive treatments. A variety of methods have been developed for segmenting vessels within MRA. One class of methods is based on a statistical model, which classifies voxels within the image volume into either vascular or non-vascular class for time-of-flight MRA [1]. Another class of segmentation is based on intensity threshold where points are classified as either greater or less than a given intensity. This is the basis of the iso-intensity surface reconstruction method [2]–[4]. This method suffers from errors due to image inhomogenities in addition; the choice of the threshold level is subjective. An alternative to segmentation is axis detection known as skeletonization process, where the central line of the tree vessels is extracted based on the tubular shape of vessels [5]. Other approaches for MRA vessel segmentation is the manually defined seed locations for segmentation [6].

In this paper, we use level set method for image segmentation to improve the accuracy of the vascular segmentation. This work is a supervised classification which means that the number of classes and the class distribution are assumed to be known. Usually, the class distribution is assumed to be Gaussian with known mean and variance. In [7], classes were assumed to be phases separated by interface boundaries where each class has its corresponding level set function. A set of functionals were developed with properties of regularity. The level set function representation depends on these functionals. Each class occupies certain areas (regions) in the image. The level set function is represented based on the regions i.e. it's positive inside the region, negative outside and zero on the boundary. The classes have no common areas i.e., the intersection between classes is not allowed. The sum of lengths of the interfaces between the areas is taken in consideration. The functionals are dependent mainly on these properties and they expect to have a local minimum which is the segmented image. The change of each level set is guided by two forces, the minimal length of interfaces which is the internal force and the homogeneous class distribution which is the external one. A Partial differential equation (PDE) guides the motion of each level set [8].

In this paper, we use level sets for the segmentation of MRA. This work saves the manual initialization of level set functions. Bad initialization for these functions makes the segmentation fails. Automatic seed initialization is made for each slice of the volume by dividing the image into windows and based on the gray level we initialize a corresponding signed distance level set function for each window. After segmenting the volume, a connectivity filter is used to exploit the fact that the vascular system is a tree-like structure and makes use of the 3D computer graphics region-filling algorithm to extract the vascular tree. The used algorithm with MRA data volumes is evaluated using a phantom showing a good accuracy. The algorithm is applied on different types of MRA data sets showing good results. This approach can be extended to be not dependent only the gray level but also on the geometrical features of the segmented areas leading to more accuracy.

2. BACKGROUND

2.1. The Level Set Function

The level set function is a function defined over the image area. It is a surface which is positive inside the region, negative outside and zero on the interfaces between regions.

$$\Phi_i(x,y,t) > 0 \text{ If } x \in \Omega_i,\ \Phi_i(x,y,t) = 0 \text{ If } x \in \Gamma_i$$

$$\Phi_i(x,y,t) < 0 \text{ Otherwise.} \quad (1)$$

Where Ω_i is the region and Γ_i is the interface between two regions.

2.2. Level Set and Image Segmentation

The level set method [8] is an analytic framework for working with evolving geometries. The level set method embeds geometries into a scalar field. Its variation with time can be described with a PDE:

$$\frac{\partial \Phi_i}{\partial t} = -F \mid \nabla \Phi_i \mid, \quad (2)$$

where F is called the speed function which is application dependent.

2.3. System of Partial Differential Equations (PDE's)

The classification inspired from [7] satisfies the following three conditions:

- The partition condition:

$$F1 = \frac{\lambda}{2} \int_{\Omega} \sum_{i=1}^{K} (H_\alpha(\phi_i) - 1)^2 dx \quad , \lambda \in R^+, \quad (3)$$

K is the number of classes.

- The data term condition:

$$F2 = \sum_{i=1}^{K} e_i \int_{\Omega} H_\alpha(\phi_i) \frac{(u_o - u_i)^2}{\partial_i^2} dx\ ,\ e_i \in R\ \forall_i, \quad (4)$$

where u_i and ∂_i^2 are the mean and variance of the class 1.

- The length shortening of interfaces:

$$F3 = \sum_{i=1}^{K} \gamma_i \int_{\Omega} \delta_\alpha(\phi_i) \mid \nabla \Phi_i \mid dx, \gamma_i \in R\ \forall_i, \quad (5)$$

H function represents the Heaviside distribution function. δ Represents the Dirac distribution function. The first represents the entire region and the second represents the boundary of the region (Fig. 1). The sum $F_1+F_2+F_3$ is minimized with respect to Φ_i, we get the solution represented by (6). This solution represents the level set function variation with time. When the function approaches the steady state, it then does not change. It has positive parts, negative and zero parts. We are interested only in the positive parts. Each pixel in the positive parts belongs to the associated class of its function.

$$\Phi_i^{t+1} = \Phi_i^{t+1} - \Delta t \delta_\alpha(\Phi_i)[e_i \frac{(u_o - u_i)^2}{\partial_i^2} - \gamma_i div(\frac{\nabla \Phi_i}{\mid \nabla \Phi_i \mid})$$

$$+\lambda(\sum_{i=1}^{K} H_\alpha(\Phi_i) - 1)] \quad (6)$$

where Δt is the step in time. By this representation, the level set function formulation allows breaking and merging fronts since equation (6) contains the curvature term which is considered to be a smoothing part.

2.4. Signed Distance Function

Signed distance function is commonly used for level set schemes where the representation defined by (6) does not maintain this condition. From [9], we find that during image segmentation, it has been found that the level sets function could be changed into a non-distance function with the initial level set function defined as a signed distance function. The solution found in [10] is to re-compute the level set function periodically based on equation (7). Each n iterations this equation is applied to regularize the level set function to remain signed distance function.

$$\frac{\partial \Phi_i}{\partial t} = \mathrm{sgn}(\Phi_i)(1 - \mid \nabla \Phi_i \mid). \quad (7)$$

We find that when it's positive the information flow goes some way and when it's negative the information flow goes the other way so it always has positive and negative parts. So by this way the level set function will have a zero level through the segmentation process which means that it's signed distance.

2.5. Stability and CFL Restriction

The solution is very sensitive to the time step. Time step is selected based on Courant-Friedrichs-Levy (CFL) restriction [8]. It requires the front to across no more than one grid cell at each time step. It's calculated as follows:

$$\Delta t = \min\{\frac{\sqrt{\Phi_x^2 + \Phi_y^2}}{(\mid \Phi_x \mid + \mid \Phi_y \mid)F}\}, \quad (8)$$

giving the maximum time step that guarantees stability. The time step is calculated at each iteration of the process.

3. VOLUME SEGMENTATION ALGORITHM

3.1. Algorithm

Step 0: Initialize Φ_i for i =1: K.

Step 1: t = t + 1.
Step 2: Update each function using equation (6).
Step 3: Solve equation (7) each n iterations.
Step 4: Smooth each function and remove noise.
Step 5: if steady state is not reached, then go to **Step 1, else** go to next slice.

Step 0 is very important since bad initialization leads to bad segmentation. Automatic seed initialization is used to speed up the process and it is also less sensitive to noise. Automatic seed initialization is to divide the image into non overlapped windows of predefined size. Then the average gray level is calculated and compared to the mean of each class to specify the nearest class it belongs to. A signed distance function is initialized to each window. The connectivity filter is applied to remove the non-vessel tissues. The filter [11] exploits the fact that the vascular system is a tree-like structure.

3.2. Segmentation Quality Measurement

A 2-D phantom is designed to simulate the MRA. This phantom image contains many circles with decreasing diameters like the cerebrovascular tree shape which is a cone-shaped. Then using the level set segmentation algorithm with this image we obtain a resultant image. The segmentation accuracy (*SA*) is measured as follows.

$$SA = \frac{No.of\ Correctly\ Classified\ Pixels}{Total\ No.of\ Pixels} X\ 100\,\% \cdot \qquad (9)$$

A value of 0.94 was computed for *SA*, indicating a high quality segmentation of the phantom image.

4. RESULTS

The proposed technique has been applied to different data sets of MR angiography phase contrast and time of flight types. For each type two volumes are used to prove the accuracy of the technique. The first type of data is 117x256x256 and the second type is 93x512x512 in size. First, level sets are initialized by automatic seed initialization (Fig. 2). Automatic seed initialization is used in each slice and each slice is divided into windows of size 5x5. Where areas of light color represent the vessels and with dark color represent the non-vessel areas. An average mean is estimated for each class from the average histogram of the volume. Segmentation results are exposed to the connectivity filter to remove the non-vessel areas. Each volume is visualized to show the vascular tree Fig. 3, 4, 5 and 6.

5. CONCLUSION

We have presented a fast and accurate level set based segmentation algorithm to extract the cerebrovascular system from MR angiography. The algorithm is a supervised segmentation. A connectivity filter was used to remove tissues that form small islands in the segmented image. The use of the phantom will help provide a quantitative evaluation of the algorithm. The 2-D phantom can be modified to be a 3-D phantom simulating the whole volume leading to more accuracy. The results are promising with a good accuracy.

6. FUTURE WORK

This model can be extended to un-supervised case including a parameter estimation capability in future work. Also the 2-D phantom can be modified to be a 3-D one simulating the whole volume leading to more accuracy. Geometrical features can be added to the segmentation model to enhance the segmentation results.

REFERENCES

[1] D. L. Wilson and J. A. Noble, "*An adaptive segmentation algorithm for time-of-flight MRA data,*" IEEE Trans on Med. Imaging,vol.18,no. 10, pp. 938–945, 1999.

[2] H. E. Cline, W. E. Lorensen, R. Kikinis, and R. Jolesz, "*Three-dimensional segmentation of MR images of the head using probability and connectivity,*" Neurosurgery, vol. 14, pp. 1037–1045, 1990.

[3] S.Nakajima,H. Atsumi, and A. H. Bhalerao, et al., "*Computer-assisted surgical planning for cerebrovascular neurosurgery,*" Neurosurgery, vol. 41, pp. 403–409, 1997.

[4] H. E. Cline, W. E. Lorensen, S. P. Souza, F. A. Jolesz, R. Kikinis,G. Gerig, and T. E. Kennedy, "*3D surface rendered MR images of the brain and its vasculature,*" JCAT, vol. 15, pp. 344–351, 1991.

[5] Peter J. Yim, Peter L. Choyke, and Ronald M. Summers, "*Gray-scale skeletonization of small vessels in magnetic resonance angiography,* " IEEE Trans on Med. Imaging, vol. 19, no. 6, pp. 568–576, 2000.

[6] E. Bullitt, el al. "*Symbolic description of intracerebral vessels segmented from magnetic resonance angiograms and evaluation by comparison with X-ray angiograms,*" Medical Imag Analysis, Vol. 5; pp. 157-169, 2001.

[7] H-K. Zaho, T. Chan, B. Merriman, and S. Osher. "*A variational level set approach to multiphase motion,*" J. of Computational Physics, 127:179-195, 1996.

[8] J.A. Sethian "*Level Set Methods and Fast Marching Methods,*", Combridge University Press, USA 1996, 1999.

[9] Hongchuan Yu, Dejun Wang, Zesheng Tang "*Level Set Methods and Image Segmentation,*", IEEE, "*International Workshop on Medical Imaging and Augmented Reality*" (MIAR'01) 0-7695-1113-9/01, June 2001.

[10] M. Sussman, P. Smereka, and S. Osher. "*A level set approach for comput-ing solutions to incompressible two-phase flow,*" J. of Computational Physics, 114:146_159, 1994.

[11] Mohamed Sabry, Charles B. Sites, Aly A. Farag, Stephen Hushek, and Thomas Moriarty "*Statistical Cerebrovascular Segmentation for Phase-Contrast MRA Data,*" Proc. of the 1st International Conf. on Biomedical Engineering, Cairo, Egypt, December, 2002.

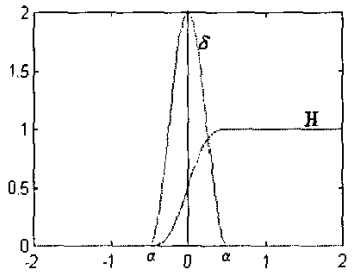

Fig 1. Plot of H and δ functions.

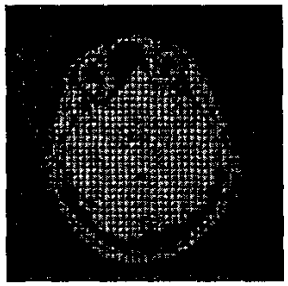

Fig. 2. Automatic Seed Initialization of slice #60 for phase Contrast MRA type.

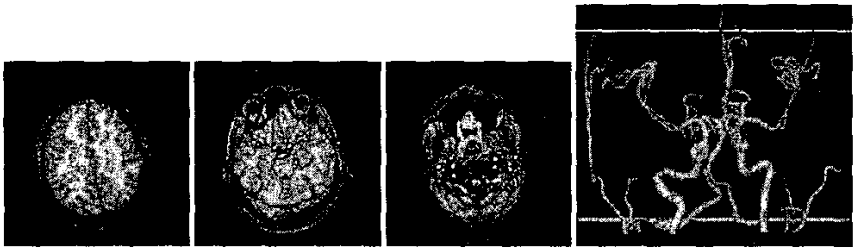

Fig. 3. Phase Contrast MRA Volume 1 Results.

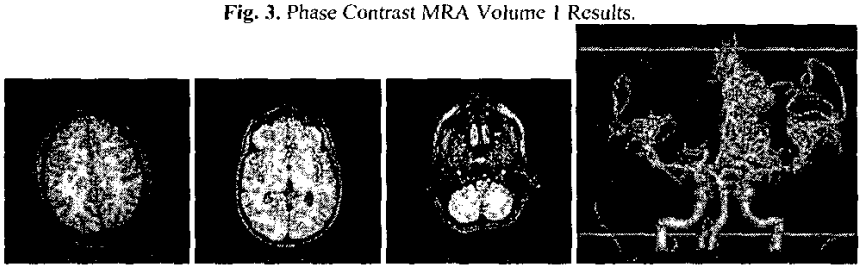

Fig. 4. Phase Contrast MRA Volume 2 Results.

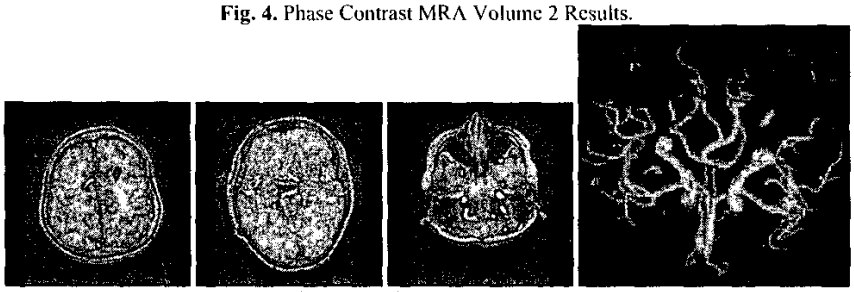

Fig. 5. Time of Flight MRA Volume 1 Results.

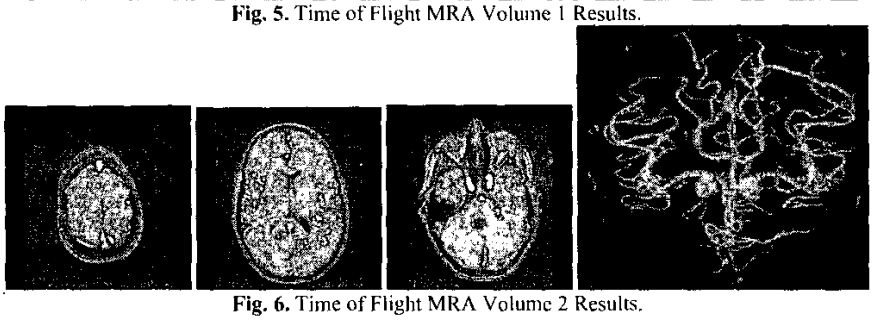

Fig. 6. Time of Flight MRA Volume 2 Results.